Letter

Excitonic Tonks-Girardeau and charge density wave phases in monolayer semiconductors

Rafał Ołdziejewski [1,2,*] Alessio Chiocchetta [3] Johannes Knörzer [1,2] and Richard Schmidt [1,2]

[1]*Max-Planck-Institute of Quantum Optics, Hans-Kopfermann-Straße 1, D-85748 Garching, Germany*

[2]*Munich Center for Quantum Science and Technology (MCQST), Schellingstrasse 4, D-80799 München, Germany*

[3]*Institute for Theoretical Physics, University of Cologne, Zülpicher Strasse 77, 50937 Cologne, Germany*

(Received 26 June 2021; accepted 15 August 2022; published 31 August 2022)

Excitons in two-dimensional semiconductors provide a novel platform for fundamental studies of many-body interactions. In particular, dipolar interactions between spatially indirect excitons may give rise to strongly correlated phases of matter that so far have been out of reach of experiments. Here we show that excitonic few-body systems in atomically thin transition-metal dichalcogenides confined to a one-dimensional geometry undergo a crossover from a Tonks-Girardeau to a charge density wave regime. To this end, we take into account realistic system parameters and predict the effective exciton-exciton interaction potential. We find that the pair-correlation function contains key signatures of the many-body crossover already at small exciton numbers and show that photoluminescence spectra provide readily accessible experimental fingerprints of these strongly correlated quantum many-body states.

DOI: 10.1103/PhysRevB.106.L081412

Introduction. Quantum systems often reveal their striking features in low spatial dimension. Prime examples include fractional excitations [1], fermionization [2] and nontrivial topology [3]. One-dimensional quantum systems offer an experimental playground to explore these rich physics using, for example, quantum optical systems such as ultracold atoms [4] and molecules [5]. Particularly, these platforms permit the study of dipolar quantum gases [6] governed by long-range magnetic interactions. Various states of matter can be explored with dipolar gases, including glass phases [7], novel superfluid [8] and supersolid phases [9–11], spin liquids [12], and exotic few-body complexes [13]. While ultracold systems benefit from high tunability, their experimental investigation is hitherto restricted to comparatively low densities or small dipole moments.

Solid-state quantum systems provide an alternative setting for realizing strongly interacting systems in reduced dimensions. Recent progress in material science and device fabrication has enabled the development of pristine low-dimensional semiconductors, which has become a versatile platform for studying quantum many-body physics [14–17]. Particularly, transition-metal dichalcogenides (TMDs) attract growing interest due to their unique optoelectronic properties [18,19]. Owing to an optical band gap and reduced screening, they enable efficient light-matter interfaces and host strongly bound excitonic quasiparticles. Exciton physics in these atomically thin nanomaterials present new possibilities for experimental study of few- and many-particle phenomena [20–26]. Notably, spatially indirect excitons feature increased lifetimes and significant electric dipole moments, making them ideally suited for studying dipolar interactions in previously unexplored parameter regimes [27–30]. Recently, electrically controlled one-dimensional (1D) confinement of in-plane excitons has been demonstrated within a single TMD monolayer [31], enabling experimental studies of dipolar excitons confined to 1D.

In this Letter we theoretically study and predict the emergence of many-body physics in a one-dimensional few-exciton system with dipolar interactions. We demonstrate that the system undergoes a crossover from a Tonks-Girardeau (TG) to a charge density wave (CDW) state even at moderate system sizes. Owing to the advantageous material properties of TMDs, the system can be operated in both regimes, depending on the exciton density. Furthermore, we find that the photoluminesence (PL) spectrum of the system contains an optical fingerprint of this crossover that can be readily probed in state-of-the-art experiments.

Setup and model. We consider a one-dimensional system of N dipolar excitons. It can be hosted both in bilayer TMDs after a careful stacking engineering or at the interface of lateral heterojunctions in monolayer TMDs [31]. Hereafter, we consider the latter, for it is conceptually simpler.[1] Here, electrons and holes are located within the single monolayer

*rafal.oldziejewski@mpq.mpg.de

[1]Note that bilayer systems offer similar prospects, as one can tune the distance between the opposite charges by stacking engineering. One could, however, devise different ways of trapping the interlayer excitons, for instance, either by trapping the center-of-mass motion or constraining the motion of individual particles to a one-dimensional wire. The specifics of the chosen realization of a 1D

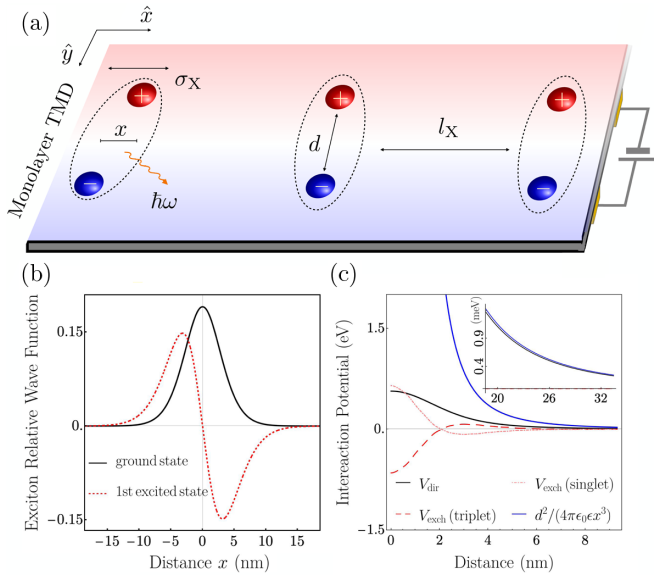

FIG. 1. (a) Sketch of the interfacial exciton system in monolayer TMDs. Electrons and holes are separated by a distance $d \sim$ (1–4) nm tuned by gate voltage. Both the electron and the hole likewise the center of mass of the resulting exciton move along a straight line. The typical distance between the excitons l_X is much larger than d and the exciton size σ_X. (b) Relative motion wave function of the ground state (solid black line) and first excited state (red dotted line) of the exciton. (c) Contributions to the calculated interaction potential between two excitons. At large distances, two excitons interact via an effective potential $V_{\rm eff}(x) \approx (ed)^2/(4\pi\varepsilon_0\epsilon x^3)$, where x is the interexciton separation.

in which they are separated via an external electric field by a distance $d \sim (1-4)$ nm that may be tuned by a gate voltage [31–33], see Fig. 1(a). Further, we assume that the typical distance between the center-of-mass (COM) coordinates of two adjacent excitons l_X is large, i.e., $l_X \gg d$. Based on recent works on interfacial excitons [31,33], we assume that the exciton wave function can be highly localized in the $\hat{y}$ direction. Under these assumptions, the exciton motion is constrained to a wire along $\hat{x}$.

Single exciton. The system of an electron and a hole is described by the Hamiltonian $H_X = -\hbar^2\partial^2_{x_e}/(2m_e) - \hbar^2\partial^2_{x_h}/(2m_h) + V_K(x_{eh})$, with $m_{e,h}$ the effective electron and hole mass, respectively, and $x_{e,h}$ the electron and hole coordinates along the wire of length L. While we assume periodic boundary conditions for simplicity, our key results also apply to fixed boundary conditions. The Rytova-Keldysh potential V_K models the dielectric screening of the Coulomb interaction [34–36], and $x_{eh} \equiv \sqrt{(x_e - x_h)^2 + d^2}$ is the distance between the electron and hole. Owing to their transversal separation, the electron and hole can be assumed to be distinguishable particles, i.e., exchange effects are neglected, as well as valence-band mixing due to spin-orbit interaction, dynamical screening, the finite width of the TMD monolayer, and the transversal motion of electrons and holes along the $\hat{y}$ direction.

setup would influence the short-range physics but not the low-density limit that we study here.

To achieve high-precision predictions of key exciton features, these and further effects would need to be included as shown in recent *ab initio* calculations based on the GW approximation [37] plus Bethe-Salpeter equation [38,39], where precise electronic-structure and dielectric considerations are included [40,41]; see also Refs. [42–50] and references therein. Our goal, however, is to study a *dilute* many-body system of excitons for which their internal structure is less relevant compared to the structure of the effective interparticle interaction, which as we will see are dominated by dipolar forces. Therefore our rather simple model for single exciton features can still serve as a qualitatively valid starting point to study the many-body properties of the system.

The eigenstates of H_X have the form $\Phi^Q_n(x_e, x_h) = \phi_n(\tilde{x})e^{iQX}/\sqrt{L}$, with $\tilde{x} = x_e - x_h$ the relative coordinate, X the center of mass, and Q the total momentum. The wave function for the relative motion of the interfacial exciton $\phi_n(\tilde{x})$ is obtained from $[-\hbar^2\partial^2_{\tilde{x}}/(2\mu) + V_K(x_{eh})]\phi_n = E_n\phi_n$, where $\mu = m_e m_h/(m_e + m_h)$ denotes the reduced mass. Figure 1(b) shows $\phi_n(\tilde{x})$ for the ground and first excited states, obtained from exact diagonalization using representative material parameters for $MoSe_2$ monolayers [51,52], $d = 4$ nm, and an average dielectric constant $\epsilon = 2.5$. Both states are bound. The ground-state (GS) energy is approximately 108 meV, and the gap to the first excited state is ∼30 meV. The width of the ground-state wave function is $\sigma_X \approx d \approx 4.7$ nm.[2],[3]

Two excitons. Due to their large binding energy and long lifetime, the interfacial excitons characterized above are ideal building blocks for studying the many-body physics of interacting bosons in TMDs. A key ingredient for their description is the derivation of the interexciton interaction potential, which we model using an approach applied to bulk semiconductors [53–59] and, recently, to monolayer TMDs [60]; for details see [36,61]. At low carrier density and temperature, the system is governed predominantly by low-energy scattering, and the mutual interactions $\hat{V}_{\rm int}$ between the fermionic constituents of the excitons can be treated as a perturbation to a system of two noninteracting excitons. Moreover, at sufficiently large interexciton separation, one may assume only the GS exciton is occupied owing to the large gap to the first excited state. Under these conditions, the COM momenta of excitons are small. Consequently, we consider the scattering of two ground-state excitons focusing only on leading terms in the effective potential as given by the Hartree-Fock and Born approximations. Assuming excitons have the same parallel spin projections, the scattering process schematically reads $(GS, Q) + (GS, Q') \xrightarrow{V_{\rm eff}(q)} (GS, Q+q) + (GS, Q'-q)$ [36]. Here, $V_{\rm eff}(q)$ is the sought-after effective potential, and q denotes the exchange momentum between the excitons. The effective potential $V_{\rm eff}(q) = V_{\rm dir}(q) + V_{\rm exch}(q)$ consists of a direct part $V_{\rm dir}$ that relates to the classical interaction between two electric dipoles and the bosonic exchange of the excitons, while $V_{\rm exch}$ accounts for fermionic exchanges between the holes and electrons.

[2]We define σ_X as the FWHM of $|\phi_{GS}(\tilde{x})|^2$.

[3]Note that our findings are in a qualitative agreement with a more detailed treatment of single interfacial excitons [33].

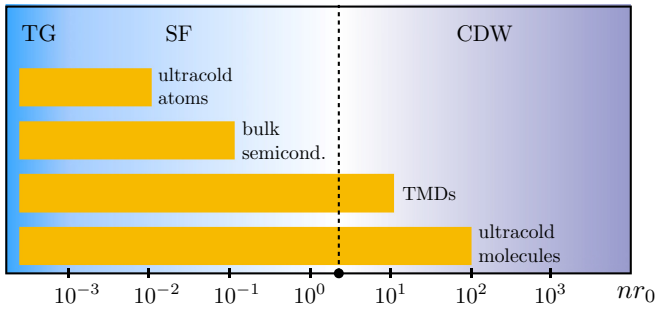

FIG. 2. Illustration of the zero-temperature phase diagram of a one-dimensional dipolar quantum gas and a comparison of its accessibility using different experimental platforms based on [62–65] and the present study of TMDs. TMDs can be expected to outperform ultracold atomic gases (e.g., Cr, Er, and Dy) and bulk semiconductors (e.g., GaAs) and complement ultracold molecules.

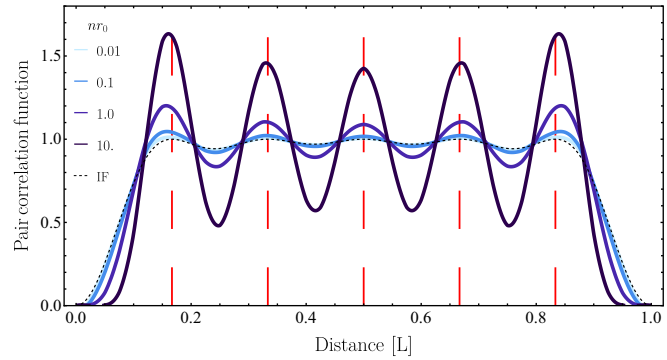

FIG. 3. Pair-correlation function as a function of distance at fixed exciton number $N = 6$ for different nr_0 tuned by adjusting the system size L. The result for ideal fermions (IFs) is recovered in the TG limit for $nr_0 \to 0$.

In Fig. 1(c) we present the contributions to the total exciton-exciton interaction, $V_{\rm dir}(x)$ and $V_{\rm exch}(x)$, for different spin states of fermions. At large distances, the direct part of the interaction reduces to the classical dipolar potential $V_{\rm dir}(x) \xrightarrow{x\to\infty} A(ed)^2/(4\pi\varepsilon_0\epsilon x^3)$ [see the inset in Fig. 1(c)], slightly decreased in strength by a factor $A \lesssim 1$ resulting from both corrections to the Coulomb interactions in the Keldysh potential and the finite extent of the exciton wave function. Due to the interfacial character of the excitons, the exchange part contributes to the effective potential only at short distances and decays exponentially. For $d \approx (1-4)$ nm, we find that the range of the exchange potential $r_{\rm exch}$ is of the same order as the size of the ground state, $r_{\rm exch} \sim \sigma_X$. It thus can be neglected, i.e., $V_{\rm eff}(x) = V_{\rm dir}(x)$ ($l_{\rm X} = n^{-1} = L/N \gg \sigma_{\rm X}$).[4] Crucially, one can check *a posteriori* that the interaction energy per particle in the many-body system does not exceed a few meV, thus confirming the validity of our assumptions.

Many excitons. Hitherto, we have argued that ground-state interfacial excitons can be treated as rigid bosons with mass $m_X = m_e + m_h$ with internal structure robust against mutual interactions. Now we investigate N such particles moving in a periodic wire of length L. This effective 1D system is governed by the Hamiltonian

$$H = -\frac{\hbar^2}{2m_X}\sum_{i=1}^{N}\frac{\partial^2}{\partial x_i^2} + \sum_{i<j}^{N} V_{\rm eff}(x_i - x_j), \qquad (1)$$

with x_i denoting the exciton coordinates.

At low temperatures, the properties of the exciton wire are encoded in the ground state of Eq. (1). Given the dipolar character of $V_{\rm eff}(x)$ at intermediate and large distances, insight into the ground state can be gained from investigating ultracold dipolar gases [62–65]. The phase diagram is controlled by the single dimensionless parameter nr_0, where the dipolar length $r_0 = m_X(ed)^2/(2\pi\hbar^2\varepsilon_0\epsilon)$ characterizes the dipolar interaction strength[5] and $n = N/L$ the 1D density of excitons. In the thermodynamic limit, the system undergoes a crossover from a TG state at low density ($nr_0 \to 0$) via a strongly correlated superfluid (SF) at intermediate nr_0 to a CDW state at large densities, see Fig. 2. In TMDs all regimes are accessible: for $MoSe_2$, $d \sim (1-4)$ nm, and $\epsilon \sim 2.5$, we find $r_0 = (20\text{–}320)$ nm. To realize the dilute regime, exciton densities in the system have to fulfill $n^{-1} \gg \sigma_{\rm X}$, implying $n \lesssim 10^6\,{\rm cm}^{-1}$, corresponding to a two-dimensional density $n_{\rm 2D} \lesssim 10^{12}\,{\rm cm}^{-2}$, consistent with typical exciton densities in TMDs [66]. Therefore experiments can, in principle, reach up to $nr_0 \lesssim 32$. As illustrated in Fig. 2, TMDs can thus outperform most alternative experimental platforms and complement studies using ultracold molecules that have yet to reach the required control to realize their full potential. We further discuss and summarize the range of realizable values of nr_0 for different classes of TMDs in the Supplemental Material [36].

Using currently available nanofabrication techniques, excitons will be trapped in finite-size systems so that only systems containing a finite number of excitons are accessible experimentally [24–26]. In the following we show that the TG-CDW crossover leaves its fingerprints in excitonic wires even in such few-body systems, where the exciton density can be controlled by laser intensity. To theoretically study this scenario, we evaluate the many-body eigenstates of the Hamiltonian (1) using exact diagonalization [36].

One quantity signaling the TG-CDW crossover [62,67] is provided by the pair-correlation function

$$g^{(2)}(x) = \frac{\langle\psi^\dagger(0)\psi^\dagger(x)\psi(x)\psi(0)\rangle}{\langle\psi^\dagger(x)\psi(x)\rangle\langle\psi^\dagger(0)\psi(0)\rangle}, \qquad (2)$$

with $\psi(x)$ and $\psi^\dagger(x)$ the exciton annihilation and creation operators in real space. In Fig. 3 we show $g^{(2)}(x)$ for a

[4]Note that this requirement holds independently of the underlying model of a single interfacial exciton. A more detailed description of electron-hole interaction (see, e.g., [49]) would only change the value of σ. Moreover, the size of the exciton is comparable to d also for a more accurate model such as discussed in Ref. [33].

[5]Note that, in general, $V_{\rm dipolar}(x) = \frac{C_{\rm dd}}{4\pi}\frac{1}{x^3}$, and thus $r_0 = \frac{mC_{\rm dd}}{2\pi\hbar^2}$. The interaction strength depends on the dipolar interaction origin (magnetic vs electric dipoles).

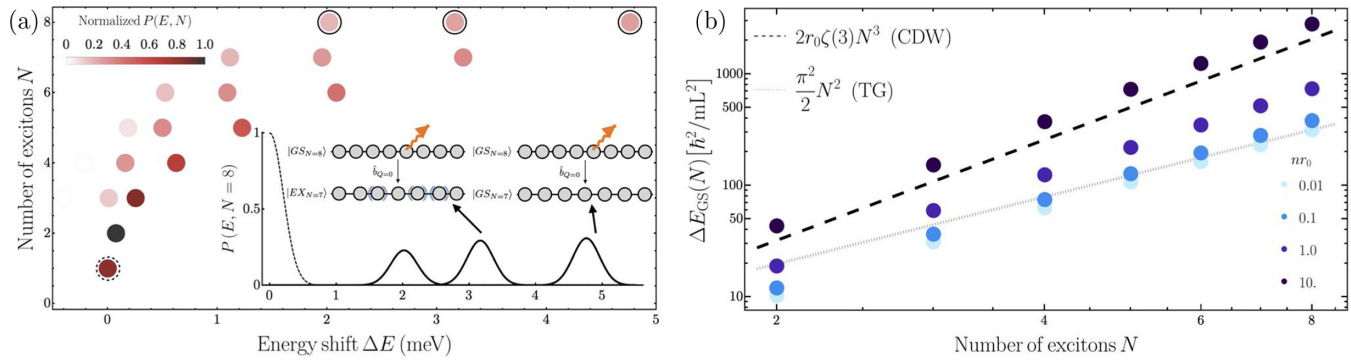

FIG. 4. (a) Photoluminescence (PL) spectrum as function of detuning from the bare exciton resonance at fixed system size $L = 156$ nm and dipolar length $r_0 = 280$ nm that for $N = 6$ yields $nr_0 = 10$. Only the most dominant PL peaks are shown, the strongest corresponding to a ground-to-ground state transition $|GS_N\rangle \to |GS_{N-1}\rangle$, while the rest originates from exciton decays, leading to excited states of the systems. Inset: The PL spectrum for $N = 8$ (solid line). The bare exciton resonance is shown as a dashed line. (b) Blue shift $\Delta E_{GS}(N) = E_{GS}(N) - E_{GS}(N-1)$ of the ground-to-ground state transition for $r_0 = 280$ nm as a function of N for different values of nr_0 (values in the legend calculated for $N = 6$).

fixed number of $N = 6$ excitons for different values of nr_0 by tuning the size of the system L. Crucially, even at such low particle numbers the observed features are in qualitative agreement with those of dipolar ultracold bosons in extended systems [62,67]. For $x \to 0$, $g^{(2)}(x)$ vanishes independently of the value of nr_0, as a consequence of the strong repulsive interaction at short range. For small nr_0, the function $g^{(2)}(x)$ approaches unity for increasing x, with small superimposed Friedel-type oscillations. The function is nearly indistinguishable from that for free fermions, reflecting that excitons are fermionized in the TG regime and exhibit a liquidlike character. For larger nr_0, the oscillations increase in magnitude, signaling the emerging crystalline CDW phase. The positions of the peaks almost coincide with the lattice sites in the solid phase (corresponding to $nr_0 \to \infty$), shown as dashed vertical lines in Fig. 3.

While this result shows that one can observe the crossover in a few-body system ($N = 6$), $g^{(2)}(x)$ is challenging to access with current experimental techniques. Thus the question arises as to which other indirect observable might provide a probe of the TG-to-CDW crossover. We hence shift our focus to another distinct signature of the phases in a 1D dipolar gas. A straightforward, analytical analysis for a large system reveals that the GS energy exhibits two limiting cases. As shown in [36], for the TG state the GS energy shows a scaling with exciton number, $E_{GS}(N) \sim N^3$ [68], that is distinct from the CDW state where $E_{GS}(N) \sim N^4$ is found. As we demonstrate in the following, these different scalings manifest themselves already at small exciton numbers in PL spectra that are readily accessible in experiments.

The photoluminescence spectrum. In TMDs, optical emission is one of the prime exciton decay mechanisms when exciton densities are sufficiently low to avoid Auger processes. The probability of emission of a PL photon is the highest for excitons with center-of-mass momentum inside the light cone, i.e., $Q \sim 0$ [69]. Since the typical equilibration time of the system is much shorter than the lifetime of an interfacial exciton, this allows us to model the PL spectra within Fermi's golden rule as

$$P(E,N) \sim \sum_k |\langle k_{N-1}|\hat{b}_{Q=0}|GS_N\rangle|^2 \delta(E - E_{GS}(N) + E_k), \tag{3}$$

with $\hat{b}_Q$ the exciton annihilation operator at momentum Q, E the energy detuned from the bare exciton resonance, $|GS_N\rangle$ the GS of the system of energy $E_{GS}(N)$ containing N excitons, $|k_{N-1}\rangle$ the eigenstates (including the GS) of the system with $N-1$ excitons, and E_k the corresponding energies.

In Fig. 4(a) we present the dominant peaks in the PL spectra upon varying the total exciton number N for fixed system size L. The system size is chosen such that for $N = 6$, one obtains a dimensionless interaction parameter $nr_0 = 10$ [6]. In the inset we show as an example an individual PL spectrum $P(E,N)$ for $N = 8$. The observed structure holds for all densities: we observe a blue shift due to the repulsive interaction, and the most probable transition corresponds to $|GS_N\rangle \to |GS_{N-1}\rangle$, while the other peaks are related to transitions to low-lying excitations of the system. We observe that the blue shift given by $\Delta E_{GS}(N) = E_{GS}(N) - E_{GS}(N-1)$ increases for larger densities with a nonlinear dependence. Similar blueshifting emissions with increasing exciton density have recently been observed in experiments studying a few indirect excitons confined by SiO_2 nanopillars [25,26].

In Fig. 4(b) we inspect the blue shift more closely by comparing our few-body results for different nr_0 with the limiting cases for a large system, where $\Delta E_{GS}^{TG} \sim N^2$ and $\Delta E_{GS}^{CDW} \sim N^3$ [36]. Remarkably, we observe not only a stark difference between the scaling of ΔE_{GS} for varying density but, indeed, recover the scaling behavior of the many-body system. Note that the offset of the N^3 power law can be attributed to the finite spread of the $g^{(2)}(x)$ function. The scaling behavior of the

[6]Note that for each N, we present here only the three most visible peaks. In all cases considered in this work, the fourth-strongest peak would be invisible to the eye.

PL spectra shows that already surprisingly small exciton systems are sufficient to reveal fingerprints of the underlying correlated phases governing the physics in the large-system limit.

Conclusions. We demonstrated that interfacial excitons display a dipolar Bose gas at interaction strengths unreachable for ultracold atoms or bulk semiconductors. We showed that the full crossover between a fermionized Tonks-Girardeau phase and a charge density wave phase can be realized and measured in conventional PL experiments with an already small number of excitons ($N < 10$). Our proposal can be extended to further setups using TMDs like interlayer excitons in heterostructures where the distance between opposite charges can be tuned by stacking engineering.

Our work also opens avenues for solid-state–based quantum simulation: for example, lattice effects can be implemented by superimposing Moiré patterns and interactions may be tunable using Feshbach resonances [70–72].

Acknowledgments. We thank J. Finley, A. Imamoğlu, A. Srivastava, and A. Stier for stimulating discussions. R.O., J.K., and R.S. acknowledge support by the Max Planck Society and the Deutsche Forschungsgemeinschaft (DFG, German Research Foundation) under Germany's Excellence Strategy–EXC-2111–390814868. A.C. acknowledges support by the funding from the European Research Council (ERC) under the Horizon 2020 Research and Innovation Program, Grant Agreement No. 647434 (DOQS).

[1] H. Steinberg, G. Barak, A. Yacoby, L. N. Pfeiffer, K. W. West, B. I. Halperin, and K. Le Hur, Nat. Phys. **4**, 116 (2008).
[2] M. Rigol and A. Muramatsu, Phys. Rev. Lett. **94**, 240403 (2005).
[3] M. McGinley and N. R. Cooper, Phys. Rev. Lett. **121**, 090401 (2018).
[4] C. Gross and I. Bloch, Science **357**, 995 (2017).
[5] N. Balakrishnan, J. Chem. Phys. **145**, 150901 (2016).
[6] T. Lahaye, C. Menotti, L. Santos, M. Lewenstein, and T. Pfau, Rep. Prog. Phys. **72**, 126401 (2009).
[7] W. Lechner and P. Zoller, Phys. Rev. Lett. **111**, 185306 (2013).
[8] A. Macia, G. E. Astrakharchik, F. Mazzanti, S. Giorgini, and J. Boronat, Phys. Rev. A **90**, 043623 (2014).
[9] F. Böttcher, J.-N. Schmidt, M. Wenzel, J. Hertkorn, M. Guo, T. Langen, and T. Pfau, Phys. Rev. X **9**, 011051 (2019).
[10] L. Chomaz, D. Petter, P. Ilzhöfer, G. Natale, A. Trautmann, C. Politi, G. Durastante, R. M. W. van Bijnen, A. Patscheider, M. Sohmen, M. J. Mark, and F. Ferlaino, Phys. Rev. X **9**, 021012 (2019).
[11] L. Tanzi, E. Lucioni, F. Famà, J. Catani, A. Fioretti, C. Gabbanini, R. N. Bisset, L. Santos, and G. Modugno, Phys. Rev. Lett. **122**, 130405 (2019).
[12] N. Y. Yao, M. P. Zaletel, D. M. Stamper-Kurn, and A. Vishwanath, Nat. Phys. **14**, 405 (2018).
[13] B. Wunsch, N. T. Zinner, I. B. Mekhov, S.-J. Huang, D.-W. Wang, and E. Demler, Phys. Rev. Lett. **107**, 073201 (2011).
[14] D. Van Tuan, B. Scharf, Z. Wang, J. Shan, K. F. Mak, I. Žutić, and H. Dery, Phys. Rev. B **99**, 085301 (2019).
[15] E. C. Regan, D. Wang, C. Jin *et al.*, Nature (London) **579**, 359 (2020).
[16] T. Smoleński, P. E. Dolgirev, C. Kuhlenkamp, A. Popert, Y. Shimazaki, P. Back, M. Kroner, K. Watanabe, T. Taniguchi, I. Esterlis, E. Demler, and A. Imamoglu, Nature (London) **595**, 53 (2021).
[17] Y. Zhou, J. Sung, E. Brutschea, I. Esterlis, Y. Wang, G. Scuri, R. J. Gelly, H. Heo, T. Taniguchi, K. Watanabe, G. Zaránd, M. D. Lukin, P. Kim, E. Demler, and H. Park, Nature (London) **595**, 48 (2021).
[18] S. Manzeli, D. Ovchinnikov, D. Pasquier, O. V. Yazyev, and A. Kis, Nat. Rev. Mater. **2**, 17033 (2017).
[19] G. Wang, A. Chernikov, M. M. Glazov, T. F. Heinz, X. Marie, T. Amand, and B. Urbaszek, Rev. Mod. Phys. **90**, 021001 (2018).
[20] M. Sidler, P. Back, O. Cotlet, A. Srivastava, T. Fink, M. Kroner, E. Demler, and A. Imamoglu, Nat. Phys. **13**, 255 (2017).
[21] E. Courtade, M. Semina, M. Manca, M. M. Glazov, C. Robert, F. Cadiz, G. Wang, T. Taniguchi, K. Watanabe, M. Pierre, W. Escoffier, E. L. Ivchenko, P. Renucci, X. Marie, T. Amand, and B. Urbaszek, Phys. Rev. B **96**, 085302 (2017).
[22] T. Mueller and E. Malic, npj 2D Mater. Appl. **2**, 29 (2018).
[23] L. Sigl, F. Sigger, F. Kronowetter, J. Kiemle, J. Klein, K. Watanabe, T. Taniguchi, J. J. Finley, U. Wurstbauer, and A. W. Holleitner, Phys. Rev. Research **2**, 042044(R) (2020).
[24] M. Förg, A. S. Baimuratov, S. Y. Kruchinin, I. A. Vovk, J. Scherzer, J. Förste, V. Funk, K. Watanabe, T. Taniguchi, and A. Högele, Nat. Commun. **12**, 1656 (2021).
[25] W. Li, X. Lu, S. Dubey, L. Devenica, and A. Srivastava, Nat. Mater. **19**, 624 (2020).
[26] M. Kremser, M. Brotons-Gisbert, J. Knörzer, J. Gückelhorn, M. Meyer, M. Barbone, A. V. Stier, B. D. Gerardot, K. Müller, and J. J. Finley, npj 2D Mater. Appl. **4**, 8 (2020).
[27] M. M. Fogler, L. V. Butov, and K. S. Novoselov, Nat. Commun. **5**, 4555 (2014).
[28] E. V. Calman, M. M. Fogler, L. V. Butov, S. Hu, A. Mishchenko, and A. K. Geim, Nat. Commun. **9**, 1895 (2018).
[29] Z. Wang, D. A. Rhodes, K. Watanabe, T. Taniguchi, J. C. Hone, J. Shan, and K. F. Mak, Nature (London) **574**, 76 (2019).
[30] C. Anton-Solanas, M. Waldherr, M. Klaas, H. Suchomel, T. H. Harder, H. Cai, E. Sedov, S. Klembt, A. V. Kavokin, S. Tongay, K. Watanabe, T. Taniguchi, S. Höfling, and C. Schneider, Nat. Mater. **20**, 1233 (2021).
[31] D. Thureja, A. Imamoglu, A. Popert, K. Watanabe, T. Taniguchi, D. J. Norris, M. Kroner, and P. A. Murthy, Nature (London) **606**, 298 (2022).
[32] P. Soubelet, J. Klein, J. Wierzbowski, R. Silvioli, F. Sigger, A. V. Stier, K. Gallo, and J. J. Finley, Nano Lett. **21**, 959 (2021).
[33] K. W. Lau, Calvin, Z. Gong, H. Yu, and W. Yao, Phys. Rev. B **98**, 115427 (2018).
[34] P. Cudazzo, I. V. Tokatly, and A. Rubio, Phys. Rev. B **84**, 085406 (2011).
[35] D. Van Tuan, M. Yang, and H. Dery, Phys. Rev. B **98**, 125308 (2018).
[36] See Supplemental Material at http://link.aps.org/supplemental/10.1103/PhysRevB.106.L081412 for additional information about details of the derivation of the exciton-exciton interaction potential, derivation of analytical expressions for the

blueshifts in the photoluminescence spectrum for different phases, numerical details of exact diagonalization, and analysis of the phase diagram for different material parameters of TMDs.

[37] M. S. Hybertsen and S. G. Louie, Phys. Rev. B **34**, 5390 (1986).
[38] M. Rohlfing and S. G. Louie, Phys. Rev. Lett. **81**, 2312 (1998).
[39] S. Albrecht, L. Reining, R. Del Sole, and G. Onida, Phys. Rev. Lett. **80**, 4510 (1998).
[40] S. Ismail-Beigi, Phys. Rev. B **73**, 233103 (2006).
[41] M. L. Trolle, T. G. Pedersen, and V. Véniard, Sci. Rep. **7**, 39844 (2017).
[42] A. Ramasubramaniam, Phys. Rev. B **86**, 115409 (2012).
[43] H.-P. Komsa and A. V. Krasheninnikov, Phys. Rev. B **86**, 241201(R) (2012).
[44] D. Y. Qiu, F. H. da Jornada, and S. G. Louie, Phys. Rev. Lett. **111**, 216805 (2013).
[45] A. Molina-Sánchez, D. Sangalli, K. Hummer, A. Marini, and L. Wirtz, Phys. Rev. B **88**, 045412 (2013).
[46] F. Hüser, T. Olsen, and K. S. Thygesen, Phys. Rev. B **88**, 245309 (2013).
[47] H. Shi, H. Pan, Y.-W. Zhang, and B. I. Yakobson, Phys. Rev. B **87**, 155304 (2013).
[48] R. Soklaski, Y. Liang, and L. Yang, Appl. Phys. Lett. **104**, 193110 (2014).
[49] D. Y. Qiu, F. H. da Jornada, and S. G. Louie, Phys. Rev. B **93**, 235435 (2016).
[50] B. Scharf, D. Van Tuan, I. Žutić, and H. Dery, J. Phys.: Condens. Matter **31**, 203001 (2019).
[51] I. Kylänpää and H.-P. Komsa, Phys. Rev. B **92**, 205418 (2015).
[52] C. Fey, P. Schmelcher, A. Imamoglu, and R. Schmidt, Phys. Rev. B **101**, 195417 (2020).
[53] C. Ciuti, V. Savona, C. Piermarocchi, A. Quattropani, and P. Schwendimann, Phys. Rev. B **58**, 7926 (1998).
[54] F. Tassone and Y. Yamamoto, Phys. Rev. B **59**, 10830 (1999).
[55] J.-i. Inoue, T. Brandes, and A. Shimizu, Phys. Rev. B **61**, 2863 (2000).
[56] S. Ben-Tabou de-Leon and B. Laikhtman, Phys. Rev. B **63**, 125306 (2001).
[57] S. Okumura and T. Ogawa, Phys. Rev. B **65**, 035105 (2001).
[58] C. Schindler and R. Zimmermann, Phys. Rev. B **78**, 045313 (2008).
[59] A. D. Meyertholen and M. M. Fogler, Phys. Rev. B **78**, 235307 (2008).
[60] V. Shahnazaryan, I. Iorsh, I. A. Shelykh, and O. Kyriienko, Phys. Rev. B **96**, 115409 (2017).
[61] T. Hahn, Comput. Phys. Commun. **168**, 78 (2005).
[62] A. S. Arkhipov, G. E. Astrakharchik, A. V. Belikov, and Y. E. Lozovik, JETP Lett. **82**, 39 (2005).
[63] R. Citro, E. Orignac, S. De Palo, and M. L. Chiofalo, Phys. Rev. A **75**, 051602(R) (2007).
[64] R. Citro, S. D. Palo, E. Orignac, P. Pedri, and M.-L. Chiofalo, New J. Phys. **10**, 045011 (2008).
[65] M. Dalmonte, G. Pupillo, and P. Zoller, Phys. Rev. Lett. **105**, 140401 (2010).
[66] L. B. Tan, O. Cotlet, A. Bergschneider, R. Schmidt, P. Back, Y. Shimazaki, M. Kroner, and A. İmamoğlu, Phys. Rev. X **10**, 021011 (2020).
[67] M. Knap, E. Berg, M. Ganahl, and E. Demler, Phys. Rev. B **86**, 064501 (2012).
[68] M. Girardeau, J. Math. Phys. **1**, 516 (1960).
[69] V. Savona, C. Piermarocchi, A. Quattropani, P. Schwendimann, and F. Tassone, Phase Transitions **68**, 169 (1999).
[70] N. Takemura, S. Trebaol, M. Wouters, M. T. Portella-Oberli, and B. Deveaud, Nat. Phys. **10**, 500 (2014).
[71] C. Kuhlenkamp, M. Knap, M. Wagner, R. Schmidt, and A. Imamoglu, Phys. Rev. Lett. **129**, 037401 (2022).
[72] M. Wagner *et al.* (unpublished).